PHYSICAL REVIEW FLUIDS **1**, 052402(R) (2016)

Sensitivity of flow evolution on turbulence structure

Aashwin A. Mishra* and Gianluca Iaccarino
Center for Turbulence Research, Stanford University, Stanford, California 94305, USA

Karthik Duraisamy
Aerospace Engineering Department, University of Michigan, Ann Arbor 48109, USA

(Received 17 May 2016; published 26 September 2016)

Reynolds averaged Navier-Stokes models represent the workhorse for studying turbulent flows in academia and in industry. Such single-point turbulence models have limitations in accounting for the influence of the nonlocal physics and flow history on turbulence evolution. In this context, we investigate the sensitivity inherent in such single-point models due to their characterization of the internal structure of homogeneous turbulent flows solely by the means of the Reynolds stresses. For a wide variety of mean flows under diverse conditions, we study the prediction intervals engendered due to this coarse-grained description. The nature of this variability and its dependence on parameters such as the mean flow topology, the initial Reynolds stress tensor, and the relative influence of linear contra nonlinear physics is identified, analyzed, and explicated.

DOI: 10.1103/PhysRevFluids.1.052402

I. INTRODUCTION

Reynolds averaged Navier-Stokes (RANS) models represent the pragmatic recourse for complex engineering flows, with a vast majority of simulations resorting to this avenue while studying turbulence. However, it is well recognized that the RANS modeling paradigm has significant shortcomings. In addition to the well-recognized issues of predictive fidelity and realizability for select flows, such models have an inherent degree of uncertainty associated with their predictions for all flows. All three of these issues arise due to shortcomings in the closure expressions. Vis-à-vis the uncertainty in predictions, the underlying sources can be divided into three levels of hierarchy.

The choice of a Markovian closure. While the evolution of the stochastic velocity field governed by the Navier-Stokes equations is Markovian, the evolution of the Reynolds stresses is unclosed and non-Markovian at the single point and instantaneous level [1,2]. Single-point turbulence closures assume that turbulence and its evolution can be completely described in terms of a finite set of local tensors, thus foisting a Markovian model onto a non-Markovian system. This does not adequately account for the nonlocal physics or the history of the flow, causing the RANS modeling problem to be ill-defined in the sense of Hadamard [3] and introduces the primary level of uncertainty in model predictions.

The form of closure and closure expression. Termed as structural uncertainty, this arises due to the limitations and biases in the closure expression. Thus, this may differ between different paradigms of RANS closures, such as one- or two-equation models and Reynolds stress transport based second moment closures.

The nature and values of the coefficients. Classified as parameter uncertainty, the appropriation of the best-possible values of the coefficients and their functional form introduces additional uncertainty in the model framework.

Owing to the importance of this subject, a multitude of recent investigations have attempted to quantify the bounds on the uncertainty in turbulence model predictions. Cheung *et al.* [4] have utilized a Bayesian uncertainty quantification approach to study the parameter uncertainty in RANS-based

*aashwin@stanford.edu

models. Recently, a physics-based, nonparametric approach to estimate the model-form uncertainties via injecting perturbations in the Reynolds stresses has been developed [5,6]. This has been applied to engineering problems with considerable success [7,8]. Other investigations [9–11] have carried out Bayesian inversion in the context of quantifying structural uncertainties.

In this investigation, we focus on the uncertainty due to the assumption that the Reynolds stress serves as an adequate description of the state of the turbulent flow. Herein, the specification of the macrostate does not lead to a unique specification of the microstates. All turbulent flows with the same Reynolds stress need not behave identically under the same conditions. The variability arising due to this coarse-grained description of the flow is common to all single-point closures and is independent of the modeling paradigm, closure expression, or the coefficients. Consequently, the best possible single-point closure, with an optimal closure expression and set of coefficients, would still have this degree of uncertainty in its predictions. Its universal nature adds to the importance of this source of uncertainty that is hitherto unexplored.

In this Rapid Communication, we seek to address the qualitative and quantitative aspects of the uncertainty introduced into the RANS modeling problem due to this coarse level description. This involves determining the prediction intervals for the evolution of turbulence statistics for diverse flows, under varying conditions. Additionally, the nature of this uncertainty is evaluated vis-à-vis the dependence of the prediction intervals on the state of the Reynolds stress tensor, the applied mean gradient, and the normalized strain rate parameter. Furthermore, this investigation provides physics-based guidance for structural uncertainty quantification using eigenvalue perturbations.

II. MATHEMATICAL DETAILS

In homogeneous turbulence, the turbulent velocity and pressure fields can be projected into Fourier space via $u_i'(\mathbf{x},t) = \sum \hat{u}_i(\boldsymbol{\kappa},t)\exp(i\boldsymbol{\kappa}\cdot\mathbf{x})$, $p^{(r)}(\mathbf{x},t) = \sum \hat{p}(\boldsymbol{\kappa},t)\exp(i\boldsymbol{\kappa}\cdot\mathbf{x})$. In this Fourier analysis, the fluctuations are characterized in terms of the wave number vector, $\boldsymbol{\kappa}(t)$, and $\hat{\mathbf{u}}$, $\hat{p}$, the corresponding Fourier amplitudes and pressure coefficients. The Fourier amplitudes and wave number evolve due to the action of the applied mean gradient, remaining perpendicular due to the incompressibility condition.

Single-point turbulence models do not have access to the states of the individual modes and rely on the singleton statistic of the Reynolds stress tensor to represent this ensemble, $R_{ij} = \sum_\kappa \hat{u}_i^* \hat{u}_j$. For any value of the initial Reynolds stress tensor, there exist many different possible compositions of the modal ensemble, each corresponding to the same Reynolds stress tensor. These different arrangements can exhibit a diverse range of evolution that may even display diametrically opposite behavior. An analogous problem occurs in the specification of the near-wall velocity boundary conditions for Large Eddy Simulation (LES). Prior investigations in this problem have shown that detailing correct statistics up to the second order at the boundary is insufficient to obtain the correct core flow [12]. Imposition of just the mean velocities and mean turbulent stresses at the artificial boundaries leads to unsatisfactory agreement, even in simple channel flow simulations [13]. These investigations have concluded that while estimation of moments beyond the second order is unnecessary, additional information about the structure of the turbulent flow is imperative to obtain a satisfactory core flow. In a similar vein, just the specification of a finite set of local tensors does not constitute a well-posed problem for RANS modeling. At this level of description, the evolution of the real flow is nonunique. We show that there is a broad envelope of possible evolution for the system, often with diametric behavior. The RANS models, being deterministic, may (at best) replicate a singleton member from this family. At this level of specification, the disparity between the broad range of possible evolution for the real flow and the unique evolution predicted by the RANS model introduces epistemic uncertainty in the model predictions.

For the purposes of this investigation, we utilize the interacting particle representation model (IPRM) of Kassinos and Reynolds [14]. Utilizing an augmented structure tensor basis as opposed to one limited to the Reynolds stress tensor [15], the IPRM is exact in the rapid distortion limit of turbulence wherein no approximation is required. Representing the nonlinear interactions using

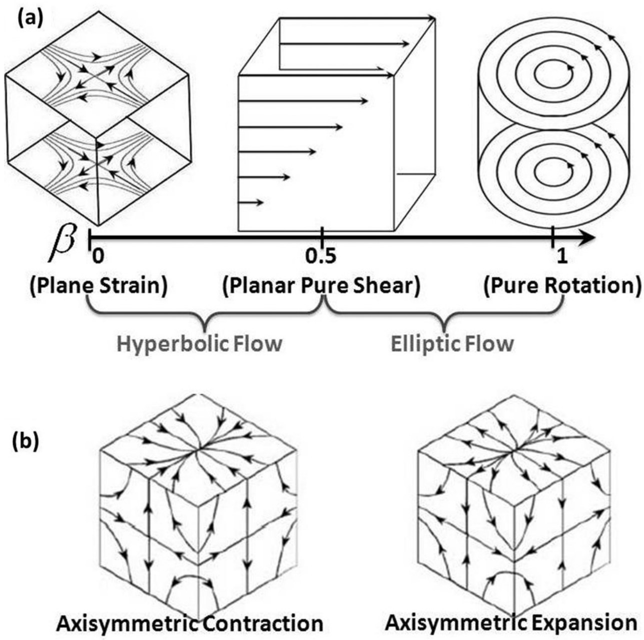

FIG. 1. Classification of flow regimes. (a) Planar quadratic flows. (b) Nonplanar flows.

a nonlocal structure-based formalism, the IPRM is able to replicate the evolution at and between the limits of weak deformations and rapid distortions. The IPRM provides accurate predictions of single-point turbulence statistics in homogeneous turbulence, for a wide variety of mean deformations at disparate values of $\frac{Sk}{\epsilon}$. For instance, the accuracy of the IPRM for the flows considered in this investigation is exhibited in detail in Kassinos and Reynolds [14,16]. Using the IPRM as our truth model, we perform a series of Monte Carlo simulations at a range of values of $\frac{\partial U_i}{\partial x_j}$, R_{ij}, and $\frac{Sk}{\epsilon}$. For each set of conditions, the simulation samples consist of over 5000 ensembles of over 20 000 individual Fourier modes. For the solution of the governing equations, we utilize the cluster formulation, outlined in Campos [17]. Herein, the Langevin evolution equations are solved for groups of realizations conditioned on a given wave vector. This is stabler than considering the Langevin evolution of individual realizations. Requisite mode and time step independence was duly carried out. As the maximum entropy distribution, Fourier amplitudes for each ensemble are sampled from a Gaussian distribution with null mean and covariance matrix corresponding to R_{ij}. For each such Fourier amplitude, the corresponding wave number vector is selected from a uniform distribution over the orthogonal plane, once again maintaining maximum entropy. Additional details of this procedure can be found in Mishra *et al.* [18] and Ledermann *et al.* [19].

For the purposes of this investigation, we restrict ourselves to certain canonical families of mean flows. The planar quadratic flows, which include cases such as plane strain, pure shear, and pure rotation, can be characterized via the ellipticity parameter: $\beta,(\frac{W_{ij}W_{ij}}{S_{ij}S_{ij}+W_{ij}W_{ij}})$ [20,21] (Fig. 1). The relative strengths of the rate of strain and rotation tensors can be ascertained by nondimensionalizing their norms by that of the mean velocity gradient tensor. In this regard, we define the derived parameters:

$$a = \sqrt{\frac{1-\beta}{2}}, \quad b = \sqrt{\frac{\beta}{2}}. \tag{1}$$

Here, the derived parameter "a" measures the relative strength of the applied strain and "b," of the applied rotation. The requisite mean flow tensors used in the simulations are given as

$$\frac{\partial U_i}{\partial x_j} = \begin{bmatrix} a & -b & 0 \\ b & -a & 0 \\ 0 & 0 & 0 \end{bmatrix}. \tag{2}$$

Thus, for the planar flows, the mean strain is restricted to the e_1-e_2 plane and the axis of rotation is aligned along the e_3 unit vector. Additionally, we study the nonplanar cases of axisymmetric contraction and expansion, where the mean gradient tensors used are given, respectively, by

$$\frac{\partial U_i}{\partial x_j} = \begin{bmatrix} S & 0 & 0 \\ 0 & -\frac{S}{2} & 0 \\ 0 & 0 & -\frac{S}{2} \end{bmatrix}, \quad \frac{\partial U_i}{\partial x_j} = \begin{bmatrix} -S & 0 & 0 \\ 0 & \frac{S}{2} & 0 \\ 0 & 0 & \frac{S}{2} \end{bmatrix}. \tag{3}$$

III. RESULTS

To characterize the uncertainty, we utilize prediction intervals, which address the range of possible evolution of the statistic at a specified level of probability, given the flow conditions and an isotropic initial state of the Reynolds stress tensor. As can be seen in the series of Figs. 2(a)–2(c), the variability in the predictions, characterized by the width of the interval, is highly dependent on the mean gradient. For hyperbolic streamline flows [Fig. 2(a)], there is a significant range of possible evolution for the turbulent kinetic energy. Additionally, this range grows exponentially with respect to time. However, for elliptic streamline flows [Fig. 2(c)], these intervals are of insignificant magnitude. At the interface of these regimes of flow for a planar sheared mean flow [Fig. 2(b)], this variability is moderately substantial and grows linearly with time. Moving from planar to three-dimensional flows, we consider the cases of a mean flow undergoing axisymmetric contraction and axisymmetric expansion. As can be seen in Figs. 3(a) and 3(b), the dependence of the predictive variability on the mean gradient is emphasized again. For the case of axisymmetric contraction, this interval remains insignificant. However, for the axisymmetric expansion mean flow, the variability is significant and exhibits growth during the phase of instability in the flow. In physical terms, for a flow undergoing axisymmetric contraction, the evolution of the flow for an isotropic state is almost independent of the internal structuring of the turbulent flow field. On the other hand, for a mean flow undergoing axisymmetric expansion, the flow evolution is highly dependent on the internal structure of the flow field.

This variability in the evolution of flow statistics is reflected in the Reynolds stress anisotropies as well. As is exhibited in Fig. 4, in a plane strain flow, there can be initially isotropic ensembles that evolve quickly where the r_{22} component contains almost all the turbulent kinetic energy, or contrarily the r_{22} component has an insignificant proportion of the turbulent kinetic energy. Furthermore, the figure exhibits that this variability in flow evolution is not just due to a select few pathological outliers. For instance, even considering a 90% prediction interval, the evolution of flow statistics can vary over orders of magnitude and can exhibit diametrically opposite behavior.

To summarize the dependence of the uncertainty on $\frac{\partial U}{\partial x}$ and $\frac{Sk}{\epsilon}$, we define a measure to characterize the uncertainty interval as $\sigma_{\mathrm{scaled}}(St) = \frac{k_{\max}(St) - k_{\min}(St)}{k_{\mathrm{mean}}(St)}$, where the turbulent kinetic energies correspond to the different sample ensembles, having the same initially isotropic Reynolds stress tensor but differing in the internal structuring of the turbulent velocity field. Scaling the range of turbulent kinetic evolution among the ensembles by the mean over the ensembles ensures that the effect of the rate of turbulent kinetic energy growth for the flow does not unduly bias the measure. As can be seen in Fig. 5, the uncertainty in predictions reduces with a decrease in the value of $\frac{Sk}{\epsilon}$. However, even at low values of this parameter, the corresponding prediction intervals are substantial.

Additionally, the magnitude of the prediction intervals depends on the initial state of the Reynolds stress anisotropies. This is exhibited in Fig. 6, for the case of a plane strain mean flow. Vis-à-vis the

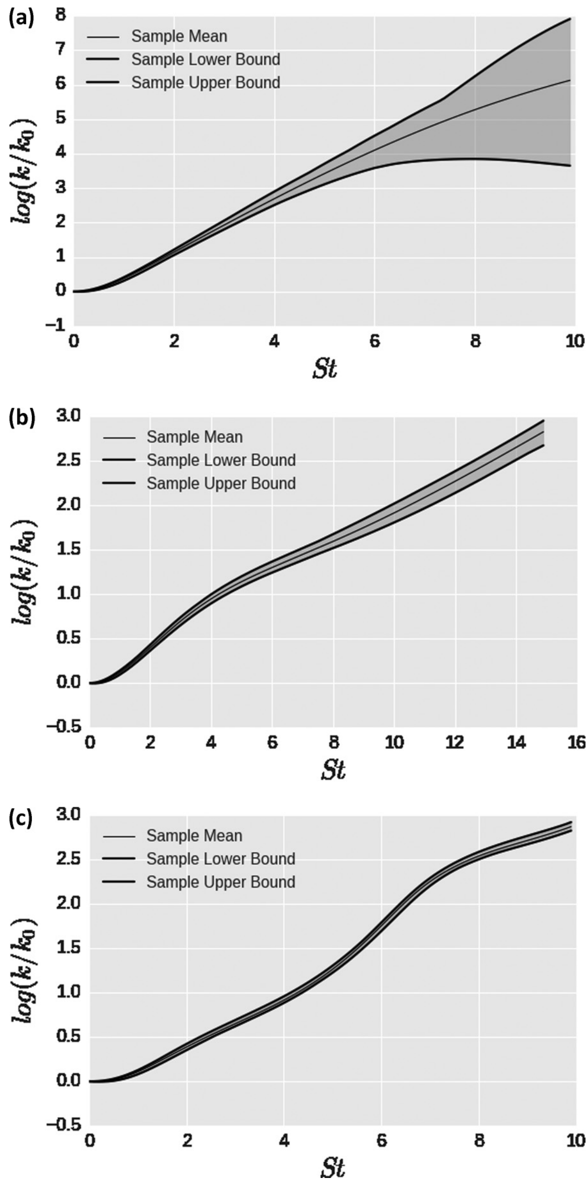

FIG. 2. Sample prediction intervals for an initially isotropic Reynolds stress at $\frac{Sk}{\epsilon} = 27$. (a) Hyperbolic flow. (b) Planar pure shear. (c) Elliptic flow.

initial state of the Reynolds stress tensor, it is found that the ordering can broadly be described as $\sigma_{1C} > \sigma_{2C} > \sigma_{3C}$.

To model the errors in RANS closures, the perturbation method of Emory *et al.* [5], Gorlé and Iaccarino [6], injects uncertainty into a spectral representation of the Reynolds stresses, thence represented as

$$R^*_{ij} = 2k^*\left(\frac{\delta_{ij}}{3} + v^*_{in}\Lambda^*_{nl}v^*_{lj}\right) \tag{4}$$

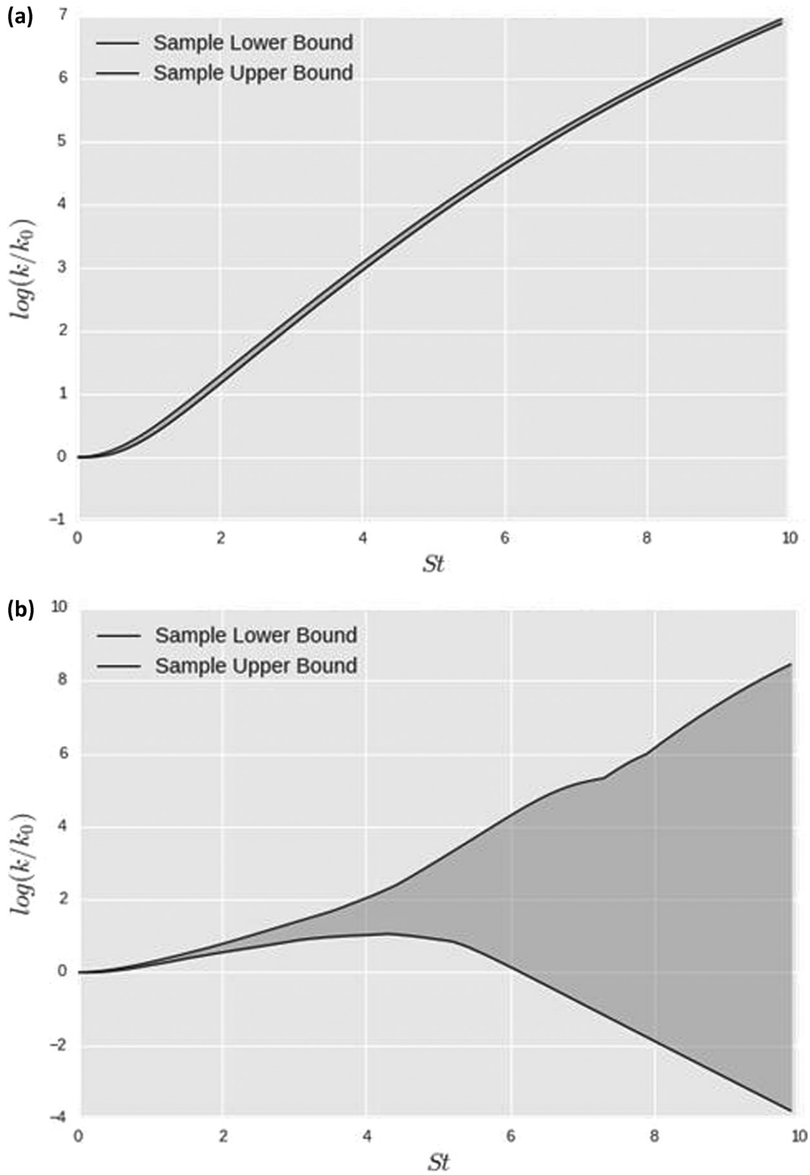

FIG. 3. Sample prediction intervals for an initially isotropic Reynolds stress at $\frac{Sk}{\epsilon} = 27$. (a) Axisymmetric contraction. (b) Axisymmetric expansion.

wherein R^*_{ij} represents the perturbed Reynolds stress; k^*, the perturbed turbulent kinetic energy; v^*, the perturbed eigenvector matrix; and Λ^*, the diagonal matrix of perturbed eigenvalues. At present, one of the key questions in such approaches is the optimal magnitude of the perturbations to the turbulent kinetic energy along with the orientation and the amplitude of the perturbations to the Reynolds stress eigenvalues. The present investigation provides distinctive guidance in this context. Based on the local mean gradient, the normalized strain rate, and flow evolution, the approximate magnitude of the perturbation to the turbulent kinetic energy can be determined, as is illustrated in Fig. 5. Additionally, based on the local state of the Reynolds stress tensor, the orientation and amplitude of eigenvalue perturbations can be ascertained, as shown in Fig. 6, to capture the extent

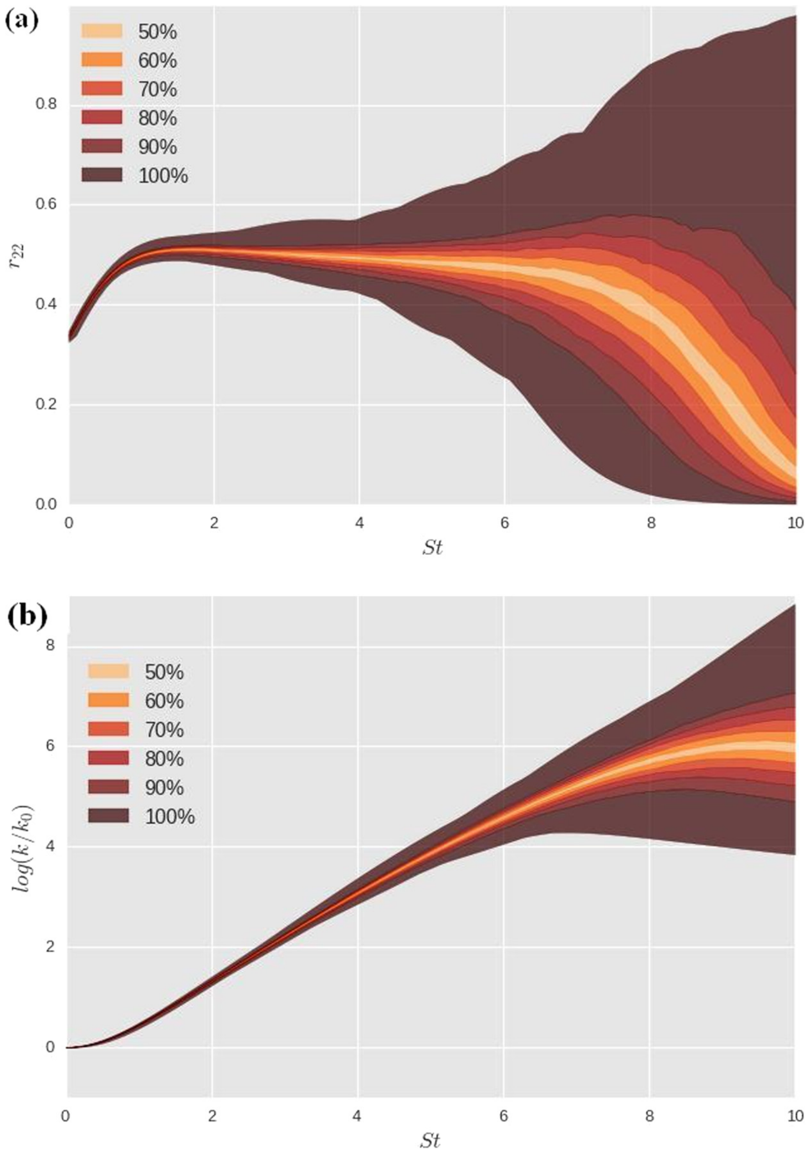

FIG. 4. Sample prediction intervals at different levels of certitude for the (a) Reynolds stress anisotropy ($r_{22} = \frac{R_{22}}{k}$) and (b) turbulent kinetic energy, k, for a plane strain mean flow (initially isotropic Reynolds stress at $\frac{Sk}{\epsilon} = 27$).

of the uncertainty in model predictions. In conjunction, these provide a systematic, physics-based recourse for the injection of uncertainty in the Reynolds stresses.

IV. DISCUSSION AND EXPLICATION

The degree of uncertainty for a particular mean flow depends on two features:

(a) The stability characteristics of the flow: The flow evolution defines a reflexive map onto the phase space of the fluctuating velocity. Clearly, a volume-expanding map will be able to exhibit a higher degree of variability than a volume-preserving (or contracting) map. In unstable flows, there is

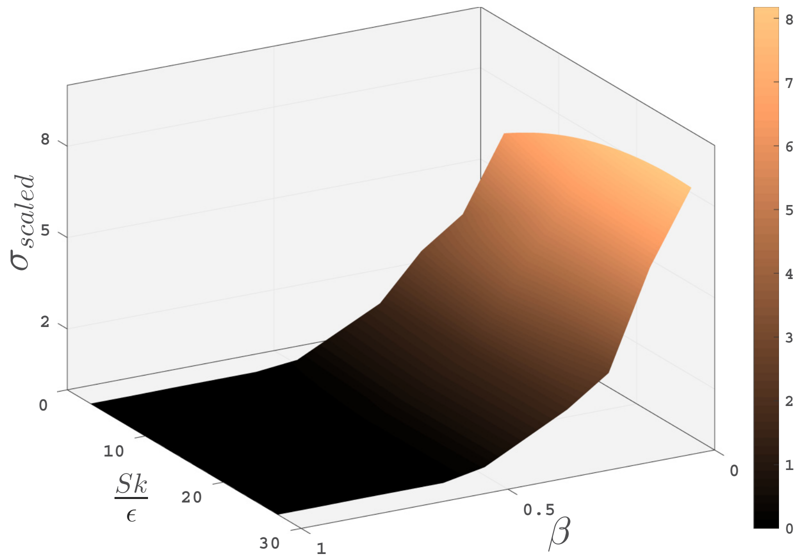

FIG. 5. Surface contours delineating the dependence of the uncertainty, quantified by σ_{scaled}, on the applied mean gradient and the strain rate parameter.

an expansion of the permissible phase space, and thus, any variability in flow evolution can increase. Consequently, the evolution of the prediction intervals depends on the nature of the instability of the flow.

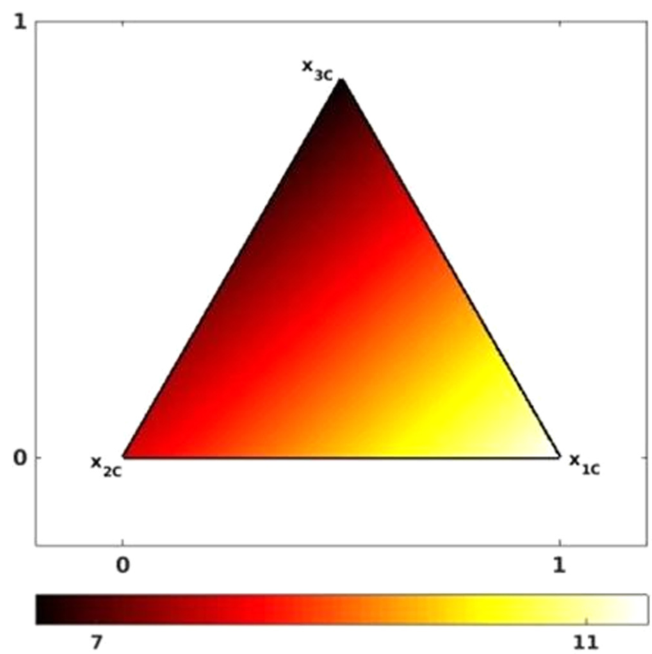

FIG. 6. Surface delineating the dependence of the uncertainty, quantified by σ_{scaled}, on the initial state of the Reynolds stress anisotropy.

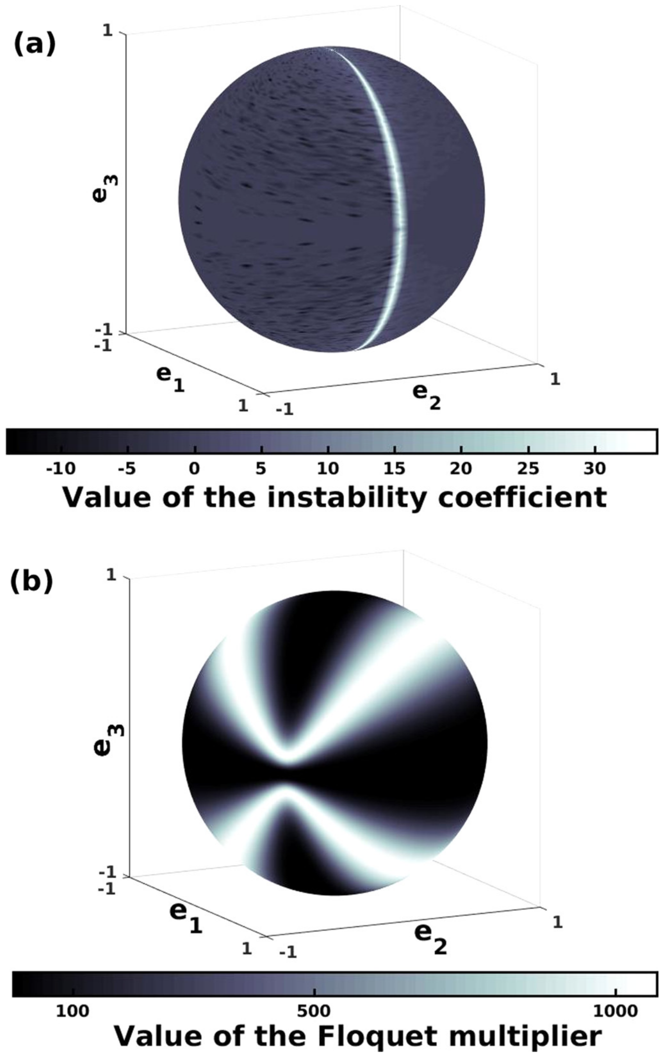

FIG. 7. Contours exhibiting the relationship between modal alignment in unit wave number space and modal stability for representative cases of (a) hyperbolic flow and (b) elliptic flow.

(b) The topology of the unstable set: In homogeneous flows, modal stability is contingent upon the alignment of the mode with respect to the applied mean gradient. Due to the structuring effect of the nonlocal action of pressure, the alignment space is divided into zones of stable and unstable alignments. A key consideration is the measure (specifically, the zero dimensionality vis-à-vis the inductive dimension) of the zones of unstable modes in unit wave number vector space.

These zones of unstable modal alignments are exhibited in Fig. 7, for different regimes of planar quadratic flows. For the hyperbolic flow, the instability coefficient is defined as $\lambda(t) = \log[k(t)/k(0)]$, where k is the turbulent kinetic energy of the flow. The Floquet multiplier as a measure of instability is described in Magnus and Winkler [22]. As can be seen, the zones of unstable modal alignments for hyperbolic flows are of zero measure, while those for elliptic flows are of finite and substantial measure. This variation is due to the fundamental difference in the physics underlying the hyperbolic and the elliptic flow instabilities. The hyperbolic flow instability is due to streamwise vortex stretching and is limited to a very small set of Fourier modes [23,24]. Thus, the evolution of hyperbolic and purely sheared flows is determined by this set of zero measure, consisting of modes that have initial alignments in these small unstable zones. Consequently, these flows are very sensitive to the internal structuring of the turbulent flow and exhibit substantial prediction intervals. For planar shear mean flows, the topology and measure of the unstable sets is homeomorphic to the hyperbolic flows. However, the flow instability exhibits polynomial growth, in contrast to the exponential growth for the hyperbolic flow cases. Thus, we observe that the prediction intervals are significant for shear flows, but grow linearly in time. The elliptic instability arises due to parametric resonance and thus, exhibits substantial bands of unstable modal alignments in wave vector space. Consequently, these flows are less sensitive to the internal structuring of the turbulent flow field. The physics underlying these instabilities and the differences in their structure in Fourier space are discussed in detail in Mishra and Girimaji [25,26].

The effect of the nonlinear physics is equivalent to the diffusion of the turbulent kinetic energy towards a uniform, isotropic distribution. This diffusion leads to an accretion in the zones of unstable modal alignments, causing them to have finite measure. This engenders a reduced sensitivity to the internal structuring of the turbulent flow for hyperbolic flows and a concomitant reduction in the prediction intervals.

V. CONCLUSIONS AND FUTURE WORK

In this Rapid Communication, we investigated the sensitivity of flow evolution on the internal structure of the turbulent flow field. Specifically, we focus on the fact that the specification of the macrostate, via the Reynolds stress tensor, does not lead to a unique specification of the microstate, the internal structuring of the turbulent flow. This lack of uniqueness leads to a variability in the evolution of the turbulent flow, causing a degree of uncertainty in the predictive fidelity of RANS models. It was exhibited that the ensuing prediction intervals are significant in magnitude and exhibit temporal growth. Their evolution and their dependence on flow parameters was analyzed and explicated. This identification provides for an *a priori*, physics-based approach toward determining eigenvalue perturbations for uncertainty quantification. In addition to its importance to the formulation of single-point RANS turbulence models, these results help guide the development of improved discrepancy models. Future work entails investigating this source of uncertainty for inhomogeneous flows and determining local time scales to compare uncertainty due to this simplification contra other sources.

ACKNOWLEDGMENT

This research was supported by the Defense Advanced Research Projects Agency under the Enabling Quantification of Uncertainty in Physical Systems (*EQUiPS*) project (technical monitor: Dr Fariba Fahroo).

[1] R. Rubinstein and S. S. Girimaji, Second moment closure near the two-component limit, J. Fluid Mech. **548**, 197 (2006).

[2] A. A. Mishra and S. S. Girimaji, Hydrodynamic stability of three-dimensional homogeneous flow topologies,Phys. Rev. E **92**, 053001 (2015).

[3] J. Hadamard, Sur les problèmes aux dérivées partielles et leur signification physique, Princeton Univ. Bull. **13**, 49 (1902).

[4] S. H. Cheung, T. A. Oliver, E. E. Prudencio, S. Prudhomme, and R. D. Moser, Bayesian uncertainty analysis with applications to turbulence modeling, Reliab. Eng. Syst. Safety **96**, 1137 (2011).

[5] M. Emory, J. Larsson, and G. Iaccarino, Modeling of structural uncertainties in Reynolds-averaged Navier-Stokes closures, Phys. Fluids (1994-present) **25**, 110822 (2013).

[6] C. Gorlé and G. Iaccarino, A framework for epistemic uncertainty quantification of turbulent scalar flux models for Reynolds-averaged Navier-Stokes simulations, Phys. Fluids (1994-present) **25**, 055105 (2013).

[7] C. García-Sánchez, D. Philips, and C. Gorlé, Quantifying inflow uncertainties for CFD simulations of the flow in downtown Oklahoma City, Building Environ. **78**, 118 (2014).

[8] C. Gorlé, C. Garcia-Sanchez, and G. Iaccarino, Quantifying inflow and RANS turbulence model form uncertainties for wind engineering flows, J. Wind Eng. Ind. Aero. **144**, 202 (2015).

[9] H. Xiao, J.-L. Wu, R. Wang, and C. Roy, Quantifying and reducing model-form uncertainties in Reynolds-averaged Navier-Stokes equations: A data-driven, physics-based, Bayesian approach, J. Comput. Phys. **324**, 115 (2016).

[10] E. Dow and Q. Wang, Quantification of structural uncertainties in the $k-\omega$ turbulence model, in *20th AIAA Computational Fluid Dynamics Conference* (American Institute of Aeronautics and Astronautics, Reston, VA, 2011), p. 3865.

[11] A. P. Singh and K. Duraisamy, Using field inversion to quantify functional errors in turbulence closures, Phys. Fluids (1994-present) **28**, 045110 (2016).

[12] J. S. Baggett, Some modeling requirements for wall models in large eddy simulation, *Annual Research Briefs* (Center for Turbulence Research, Stanford University, 1997), pp. 123–134.

[13] F. Nicoud, G. Winckelmans, D. Carati, J. Baggett, and W. Cabot, Boundary conditions for LES away from the wall, *Proceedings of the CTR Summer Program* (Center for Turbulence Research, Stanford University, 1998), pp. 413–442 .

[14] S. C. Kassinos and W. C. Reynolds, Advances in structure-based turbulence modeling, *Annual Research Briefs* (Center for Turbulence Research, Stanford University, 1997), pp. 179–193.

[15] S. C. Kassinos, W. C. Reynolds, and M. M. Rogers, One-point turbulence structure tensors, J. Fluid Mech. **428**, 213 (2001).

[16] S. C. Kassinos and W. C. Reynolds, A particle representation model for the particle deformation of homogeneous turbulence, *Annual Research Briefs* (Center for Turbulence Research, Stanford University, 1996), p. 31.

[17] A. Campos, Advances in structure-based modeling of turbulent flows, Ph.D. thesis, Stanford University, 2016.

[18] A. A. Mishra, G. Iaccarino, and K. Duraisamy, Epistemic uncertainty in statistical Markovian turbulence models, *Annual Research Briefs* (Center for Turbulence Research, Stanford University, 2015), pp. 183–195.

[19] W. Ledermann, C. Alexander, and D. Ledermann, Random orthogonal matrix simulation, Linear Algebra Appl. **434**, 1444 (2011).

[20] A. A. Mishra, The art and science in modeling the pressure-velocity interactions, Ph.D. thesis, Texas A&M University, 2014.

[21] A. A. Mishra, A dynamical systems approach towards modeling the rapid pressure strain correlation, Master's thesis, Texas A&M University, 2010.

[22] W. Magnus and S. Winkler, Hill's equation (Courier Corporation, North Chelmsford, MA, 2013) .

[23] A. A. Mishra and S. S. Girimaji, On the realizability of pressure-strain closures, J. Fluid Mech. **755**, 535 (2014).

[24] A. A. Mishra and S. S. Girimaji, Manufactured turbulence with Langevin Equations, ERCOFTAC Bull. **92**, 11 (2012).

[25] A. A. Mishra and S. S. Girimaji, Pressure-strain correlation modeling: Towards achieving consistency with rapid distortion theory, Flow, Turbul. Combust. **85**, 593 (2010).

[26] A. A. Mishra and S. S. Girimaji, Intercomponent energy transfer in incompressible homogeneous turbulence: Multi-point physics and amenability to one-point closures, J. Fluid Mech. **731**, 639 (2013).